JOURNAL OF SPACECRAFT AND ROCKETS
Vol. 38, No. 4, July–August 2001

GEOSAIL: Exploring the Geomagnetic Tail Using a Small Solar Sail

Colin R. McInnes* and Malcolm Macdonald†
University of Glasgow, Glasgow, Scotland G12 8QQ, United Kingdom
Vassilis Angelopolous‡
University of California, Berkeley, Berkeley, California 94720-7450
and
David Alexander§
Lockheed Martin Solar and Astrophysics Laboratory, Palo Alto, California 943044

Conventional geomagnetic tail missions require a spacecraft to be injected into a long elliptical orbit to explore the spatial structure of the geomagnetic tail. However, because the elliptical orbit is inertially fixed and the geomagnetic tail is directed along the sun–Earth line, the apse line of the elliptical orbit is precisely aligned with the geomagnetic tail only once every year. To artificially precess the apse line of the elliptical orbit in a sun-synchronous manner, which would keep the spacecraft in the geomagnetic tail during the entire year, would require continuous low-thrust propulsion or periodic impulses from a high-thrust propulsion system. Both of these options require reaction mass that will ultimately limit the mission lifetime. It is demonstrated that sun-synchronous apse-line precession can be achieved using only a small, low-cost solar sail. Because solar sails do not require reaction mass, a geomagnetic tail mission can be configured that provides a continuous science return by permanently stationing a science payload within the geomagnetic tail.

Nomenclature

a = semimajor axis, km
a_p = electric propulsion acceleration, mm/s^2
a_0 = solar sail characteristic acceleration at 1 astronomical unit (AU), mm/s^2
e = eccentricity
f = true anomaly, deg
m = spacecraft mass, kg
$\boldsymbol{n}$ = sail normal unit vector
p = orbit semiparameter, km
R = radial perturbing acceleration, mm/s^2
r = orbit radius, km
r_0 = 1 AU
$\boldsymbol{s}$ = sun-line unit vector
T = transverse perturbing acceleration, mm/s^2
T_0 = orbit period, s
α = sail orientation relative to the sun–Earth line, deg
λ_S = longitude of sun from vernal equinox, deg
μ = gravitational parameter, Nm^2 kg^{-2}
ϕ = thrust orientation relative to radial direction, deg
ω = argument of perigee, deg

Subscript

s = with respect to heliocentric elements

Introduction

SOLAR sailing utilizes the solar radiation pressure exerted on a large tensioned reflective membrane to provide a propulsive force without the need for reaction mass. It has long been considered as a means of enabling high-energy space science missions or enhancing existing deep space mission concepts by reducing launch mass and trip times. However, most of these mission applications have only considered solar sail propulsion as a transportation device that provides an efficient means of delivering payloads to planetary or small solar system bodies.[1] In contrast, recent work has shown that solar sails can enable new classes of missions that use the continuously available solar radiation pressure to generate families of highly non-Keplerian orbits.[2–4] These missions do not use the solar sail as a transportation device, but as a means of obtaining new observation points for solar physics, Earth observation, and space science applications. This paper investigates yet another new class of non-Keplerian orbits enabled by solar sails. These new orbits appear to have significant space physics applications and, more important, are achievable in the near term using only a small, low-performance solar sail. The use of a small solar sail offers the possibility of configuring an initial technology demonstration mission for solar sail propulsion which also provides a unique and useful science return. The GEOSAIL mission concept detailed here has been designed to achieve both of these goals.

The mission application considered centers on artificial precession of the apse line of an elliptical orbit whose major axis lies along the Earth's geomagnetic tail. The geomagnetic tail is the long structure formed by interaction of the magnetized solar wind with the magnetic field of the Earth and is a key focus of investigation for the space physics community.[5] Because a Keplerian elliptical orbit is inertially fixed and the geomagnetic tail is directed along the sun–Earth line, the apse line of such a Keplerian elliptical orbit is precisely aligned with the geomagnetic tail only once every year. Therefore, useful science data can only be gathered from the geomagnetic tail for a relatively short duration each year when the apse line of the ellipse and the geomagnetic tail are aligned. However, using a small solar sail it will be shown that the orbit apse line can be artificially precessed at 0.9856 deg/day to track precisely the annual rotation of the geomagnetic tail. Such a forced orbit enables continuous science returns during an entire year, rather than the short annual window when the apse line of the ellipse and the geomagnetic tail are aligned.

The mission orbits of interest for forced apse-line precession are related to the physical processes to be investigated. For example, a stable perigee radius of order 10 Earth radii provides sampling of

Received 6 September 2000; revision received 29 March 2001; accepted for publication 30 March 2001.

*Professor, Department of Aerospace Engineering; colinmc@aero.gla.ac.uk.

†Graduate Student, Department of Aerospace Engineering; m.macdonald@aero.gla.ac.uk.

‡Assistant Research Physicist, Space Sciences Laboratory; vassilis@SSL.Berkeley.EDU.

§Research Scientist, 3251 Hanover Street; alexander@lmsal.com.

the magnetopause on the day side of the Earth, whereas an apogee radius of order 30 Earth radii samples the magnetotail with an orbit period of 5.24 days. For apogee radii beyond 25 Earth radii, an orbit within the ecliptic plane is found to be optimum for space physics applications. The science goals of the GEOSAIL mission proposed here are to achieve long residence times in the geomagnetic tail to enable adequate statistical characterization of the plasma under a variety of solar wind conditions. By the maintainence of an essentially constant presence in the geomagnetic tail, the rapid dynamic evolution of the geomagnetic tail can be probed. In particular, so-called magnetic reconnection events are likely to be observed in situ for the first time.

First, a simple solar sail steering law is derived that provides forced apse-line precession for an elliptical orbit within the ecliptic plane. The conditions for sun-synchronous precession are then derived and solar sail performance requirements are identified for the scientifically interesting orbits discussed earlier. It will then be demonstrated that the steering law is in effect adaptive in that the precession rate of the elliptical orbit will adjust to the varying rotation rate of the sun line due to the eccentricity of the Earth's heliocentric orbit.

Forced apse-line precession using a solar sail is then compared to forced precession using low-thrust electric or high-thrust chemical propulsion. Again, performance requirements are identified for sun-synchronous apse-line precession using simple steering laws. These simple steering laws are compared to locally optimum steering laws that maximize the instantaneous rate of increase of argument of perigee. A locally optimum steering law for electric propulsion is derived, which is then adapted for use by a solar sail. It is found that these locally optimum steering laws provide only a modest advantage over the simple steering laws.

Last, a preliminary mission concept is presented, which utilizes artificial apse-line precession for a geomagnetic tail mission using a small, low-cost solar sail. A strawman payload is identified, and a total spacecraft mass is determined assuming currently available deployable boom and sail film technologies.[6] It is shown that the resulting spacecraft is suitable for launch as a secondary payload, possibly on the Ariane V auxiliary payload ring, and that the level of solar sail performance is typical of that currently being considered for near-term technology demonstration missions. Current technology demonstration mission concepts envisage a slow spiral to Earth escape or a lunar fly-past, neither of which has particular scientific merit. The mission concept proposed here allows technology demonstration of a low-cost solar sail along with a unique and useful science return. The unique science return adds to the programmatic benefits of the mission by demonstrating that solar sailing is not just an efficient means of low-thrust propulsion, but enables entirely new ways of performing science missions. The GEOSAIL mission concept detailed in this paper combines technology demonstration with a unique and useful science return.

Apse-Line Precession Using Solar Sails

For the mission orbit discussed, the solar sail will orbit within the ecliptic plane so that only three osculating orbital elements are required to describe the evolution of the resulting trajectory. The sail normal is also assumed to be directed within the ecliptic plane so that there will only be an in-plane perturbing acceleration due to solar radiation pressure. To investigate steering laws for apse-line precession the following Lagrange equations are, therefore, used[7]:

$$\frac{\mathrm{d}a}{\mathrm{d}f} = \frac{2pr^2}{\mu(1-e^2)^2}\left[Re\sin f + T\frac{p}{r}\right] \tag{1}$$

$$\frac{\mathrm{d}e}{\mathrm{d}f} = \frac{r^2}{\mu}\left[R\sin f + T\left(1+\frac{r}{p}\right)\cos f + Te\frac{r}{p}\right] \tag{2}$$

$$\frac{\mathrm{d}\omega}{\mathrm{d}f} = \frac{r^2}{\mu e}\left[-R\cos f + T\left(1+\frac{r}{p}\right)\sin f\right] \tag{3}$$

where R and T are the radial and transverse components of the perturbing solar radiation pressure acceleration experienced by the solar sail, as shown in Fig. 1, and $p = a(1-e^2)$ is the orbit semiparameter.

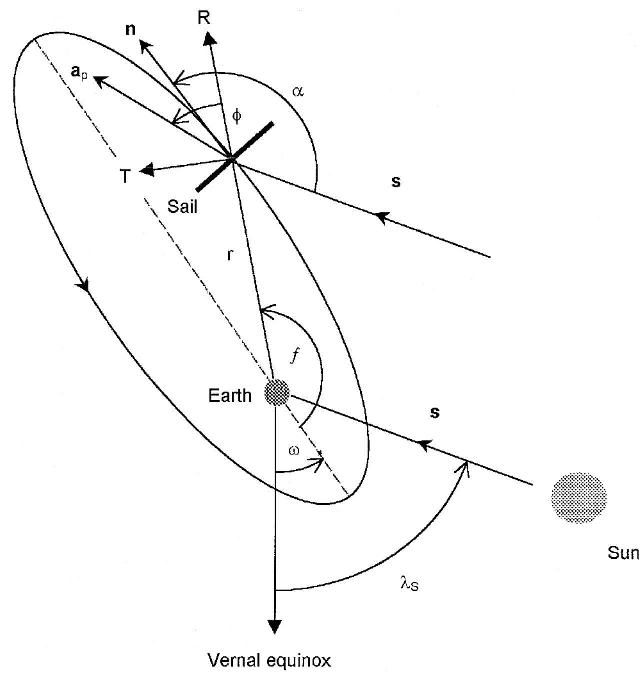

Fig. 1 Orbit geometry.

A simple steering law will now be considered in which the sail normal is directed along the major axis of the ellipse.

The solar radiation pressure acceleration experienced by the solar sail is a function of the sail orientation with respect to the sun line. If $\boldsymbol{n}$ is the unit vector normal to the sail surface and $\boldsymbol{s}$ is the unit vector directed along the sun line, the solar radiation pressure acceleration experienced by an ideal solar sail on an Earth-centered orbit may be written as $\boldsymbol{a} = a_0(\boldsymbol{s}^T\boldsymbol{n})^2\boldsymbol{n}$, where a_0 is the characteristic acceleration of the solar sail. The characteristic acceleration is defined as the acceleration experienced by the solar sail at a heliocentric distance of 1 astronomical unit (AU) while the sail normal is directed along the sun line in the antisun direction. Therefore, if the sail normal is directed along the major axis of the ellipse, the components of the solar radiation pressure acceleration experienced by the solar sail are given by

$$\begin{bmatrix} R \\ T \end{bmatrix} = a_0\cos^2(\omega-\lambda_S)\begin{bmatrix} -\cos f \\ \sin f \end{bmatrix} \tag{4}$$

where ω is the argument of perigee of the orbit, λ_S is the position of the sun within the ecliptic plane from the vernal equinox, and f is the true anomaly of the spacecraft, again shown in Fig. 1.

For the rotation of the apse line of the orbit to be synchronous with the annual rotation of the sun line, it is clear that the identity $\omega = \lambda_S$ must always hold. In this case, the sun line is directed along the major axis of the ellipse and so the sail normal is always directed along the sun line. This strategy provides an extremely simple steering law to implement in practice. The change in orbital elements over a single orbit with this simple sail steering law [Eq. (4)] can now be obtained by integrating Eqs. (1–3) to obtain

$$\Delta a = \int_0^{2\pi}\frac{\mathrm{d}a}{\mathrm{d}f}\,\mathrm{d}f = 0 \tag{5}$$

$$\Delta e = \int_0^{2\pi}\frac{\mathrm{d}e}{\mathrm{d}f}\,\mathrm{d}f = 0 \tag{6}$$

so that the orbit-averaged semimajor axis and eccentricity remain unchanged by the solar radiation pressure acceleration experienced by the solar sail. Again, integrating Eq. (3) over a single orbit with the steering law defined by Eq. (4), the change in argument of perigee of the ellipse is found to be

$$\Delta\omega = (3\pi/\mu)a_0a^2\sqrt{(1-e^2)/e^2} \tag{7}$$

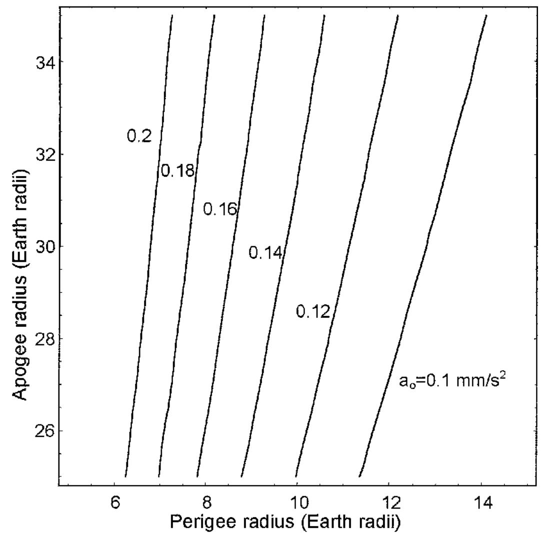

Fig. 2 Solar sail characteristic acceleration required for sun-synchronous apse-line precession (mm/s^2).

so that the apse line of the ellipse will rotate due to the perturbing solar radiation pressure acceleration. The mean rate of precession of the apse line of the ellipse can now be obtained by dividing Eq. (7) by the ellipse orbit period T_0 to obtain

$$\frac{\Delta\omega}{T_0} = \frac{3}{2}a_0\left[\frac{\sqrt{(1-e^2)}}{e}\right]\sqrt{\frac{a}{\mu}} \tag{8}$$

where $T_0 = 2\pi\sqrt{(a^3/\mu)}$. Therefore, for the sun-synchronous condition that $\Delta\omega/T_0 = \dot{\lambda}_S$, the required solar sail characteristic acceleration is found to be

$$a_0 = \tfrac{2}{3}\dot{\lambda}_S\left(e/\sqrt{1-e^2}\right)\sqrt{\mu/a} \tag{9}$$

where $\dot{\lambda}_S = 0.9856$ deg/day. Equation (9) provides a compact expression to size a solar sail for a given elliptical orbit with the condition for sun-synchronous apse-line precession.

For sun-synchronous apse-line precession, it can be seen that the required solar sail characteristic acceleration is only a function of the orbit semimajor axis and eccentricity, both of which remain unchanged over a single orbit. A convenient way of representing the required characteristic acceleration is, therefore, through the orbit apogee and perigee radii, as shown in Fig. 2. For the range of orbits of interest (near 10 × 30 Earth radii) it can be seen that a solar sail characteristic acceleration of order 0.15 mm/s^2 is required. This level of performance is typical of current concepts for near-term solar sail technology demonstration missions.[6] Note that the natural precession of the apse line due to Earth oblatness for these orbits is only of order 10^{-3} deg/day.

As already discussed, an elliptical orbit in the ecliptic plane with a perigee radius of 10 Earth radii and an apogee radius of 30 Earth radii is of interest for space physics applications. For this particular orbit, the required solar sail characteristic acceleration is obtained from Eq. (9) as 0.136 mm/s^2. The evolution of this orbit over 30 days is shown in Fig. 3. It can be seen that the orbit-averaged change in semimajor axis and eccentricity are zero as expected, while the apse line of the orbit precesses at a mean rate of 0.9856 deg/day to track the sun line and geomagnetic tail, as required. A more detailed analysis of this orbit including lunar and solar gravitational perturbations will be provided in a later section.

In the preceding analysis, a constant apse-line precession rate has been sought to provide sun-synchronous conditions. However, due to the eccentricity of the Earth's orbit about the sun, the sun line will not rotate at a uniform rate. From conservation of angular momentum, it can be shown that the sun-line rotation rate will vary as the inverse square of the planetary heliocentric distance r_s as

$$\dot{\lambda}_S = \sqrt{\mu_s a_s\left(1-e_s^2\right)}\Big/r_s^2 \tag{10}$$

where the subscript s denotes the planetary heliocentric orbital elements. However, because solar radiation pressure also has an inverse-square variation with heliocentric distance, the forced precession of the elliptical orbit apse line has the same functional relationship. From Eq. (8), the modified mean precession rate is given by

$$\langle\dot{\omega}\rangle = \tfrac{3}{2}a_0(r_0/r_s)^2\left[\sqrt{(1-e^2)}/e\right]\sqrt{a/\mu} \tag{11}$$

where r_0 is 1 AU and the term $(r_0/r_s)^2$ scales the solar radiation pressure with varying heliocentric distance. The sun-pointing steering law discussed earlier will, therefore, maintain sun-synchronous precession of the elliptical orbit apse line, even if the planetary orbit about the sun is noncircular. This effect has also been noted for other solar sail mission applications.[4] Whereas the annual variation of sun-line rotation rate is a relatively minor effect for Earth-centered orbits, it will be significant at Mercury, for example, due to the high eccentricity of Mercury's orbit.

An additional effect that has been neglected in the analysis leading to Eq. (9) is eclipse periods at the apogee of the sun-synchronous elliptical orbit. Because the orbit apse line precesses in a sun-synchronous manner, these eclipses will occur with the same duration at each orbit apogee passage. If the eclipse period spans a range of true anomaly $2\Delta f$ centered on the orbit apogee, the change in argument of perigee during a single orbit is now obtained from

$$\Delta\omega = \int_{-\pi+\Delta f}^{\pi-\Delta f}\frac{\mathrm{d}\omega}{\mathrm{d}f}\,\mathrm{d}f \tag{12}$$

Substituting from Eqs. (3) and (4) and integrating yields the change in argument of perigee during a single orbit with an eclipse of width $2\Delta f$ as

$$\Delta\omega = \frac{1}{\mu}a_0a^2\sqrt{\frac{1-e^2}{e^2}}\left[6\tan^{-1}\left(\sqrt{\frac{1-e}{1+e}}\cot\Delta f\right)\right.$$
$$\left.+\sqrt{1-e^2}\sin\Delta f\frac{(2e^2\cos\Delta f-3e+\cos\Delta f)}{(1-e\cos\Delta f)^2}\right] \tag{13}$$

which reduces to Eq. (7) in the limit $\Delta f \to 0$. For the 10 × 30 Earth radii mission orbit, the eclipse half-width $\Delta f \sim 1.9$ deg, and so the solar sail characteristic acceleration required for sun-synchronous apse-line precession increases marginally from 0.136 to 0.138 mm/s^2. It is clear from this analysis that repeated short-duration eclipses have little effect on the required solar sail performance for the range of orbits of interest.

Apse-Line Precession Using Electric and Chemical Propulsion

Forced apse-line precession is also possible using electric or chemical propulsion, although the requirement for reaction mass will limit the duration for which sun-synchronous precession can be sustained by these means. For electric propulsion, the required spacecraft acceleration can be obtained from Eq. (9) if the thrust vector is always directed along the major axis of the ellipse. An equivalent steering law can be obtained as a particular case of the analysis of Pollard[8] for electric propulsion transfer problems.

An alternative steering law is proposed by Burt,[9] in which the thrust vector of the electric propulsion system is directed along the transverse direction, but reverses sign at each crossing of the major axis of the orbit so that

$$R = 0 \tag{14}$$

$$T = \begin{cases} +a_p, & 0 \le f < \pi \\ -a_p, & \pi \le f < 2\pi \end{cases} \tag{15}$$

where a_p is the aceleration induced by the electric propulsion system. This is a seemingly more efficient means of inducing apse-line precession. When Eqs. (1–3) are used and this steering law is

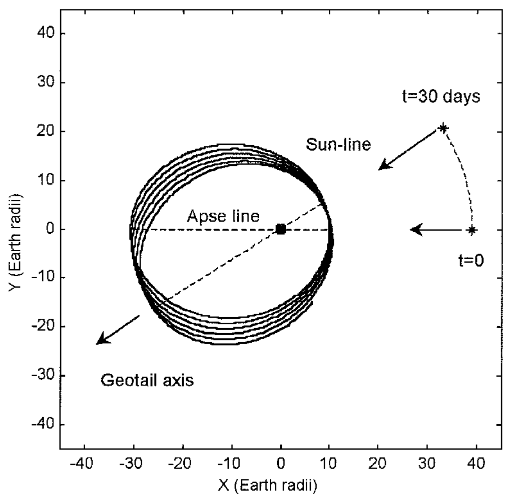

Fig. 3a Mission orbit of 10 × 30 Earth radii; evolution over 30 days.

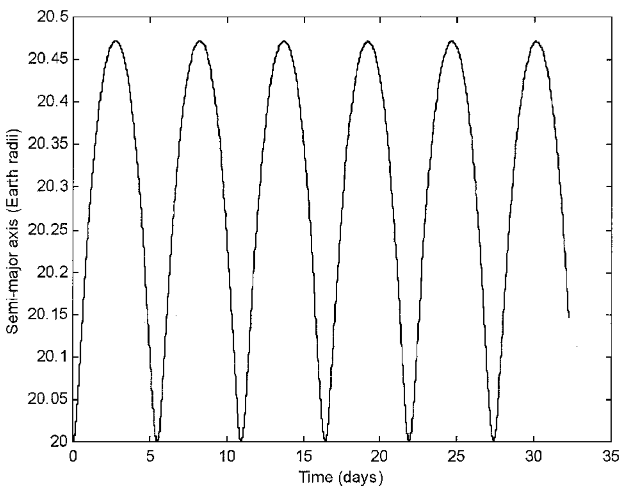

Fig. 3b Orbit semimajor axis.

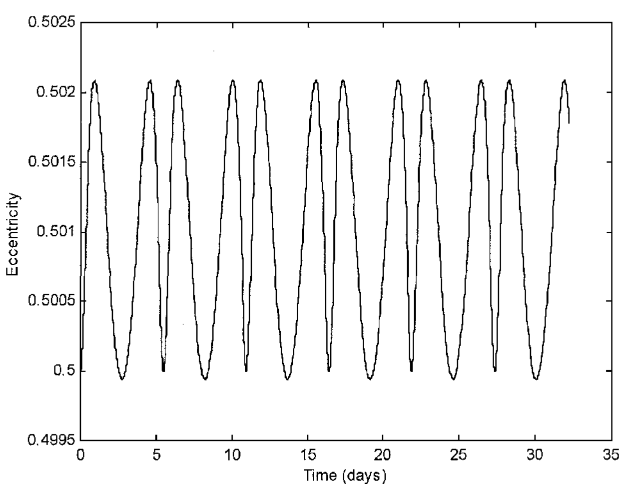

Fig. 3c Orbit eccentricity.

integrated, it can be shown that the changes in elements over a single orbit are given by

$$\Delta a = 0 \tag{16}$$

$$\Delta e = 0 \tag{17}$$

$$\Delta\omega = (4/\mu)a_p a^2[(e^2 - 2)/e] \tag{18}$$

Again, requiring sun-synchronous apse-line precession so that $\Delta\omega/T_0 = \dot{\lambda}_S$, the acceleration required from the electric propulsion system is found to be

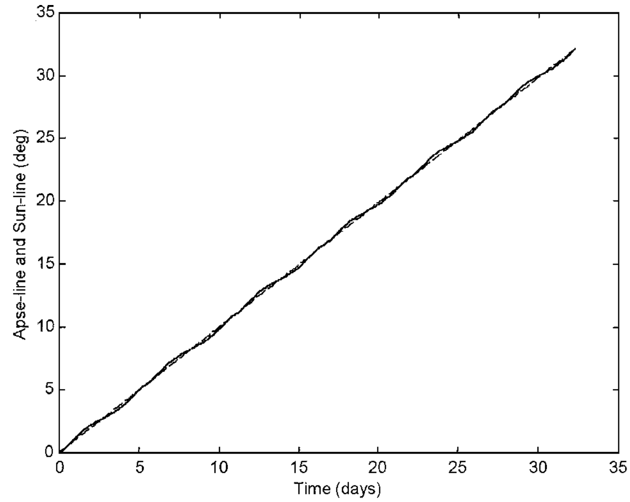

Fig. 3d Apse line ω (——) and sun line λ_S (- - -) over 30 days.

$$a_p = (\pi/2)\dot{\lambda}_S[e/(2 - e^2)]\sqrt{\mu/a} \tag{19}$$

which can be used to size the spacecraft thrusters. The steering laws of Pollard[8] and Burt[9] for electric propulsion can now be compared by equating Eqs. (9) and (19) to obtain the identity

$$2 - e^2 = (3\pi/4)\sqrt{1 - e^2} \tag{20}$$

After making the substitution $z = \sqrt{(1 - e^2)}$, a quadratic is obtained that discriminates between the two steering laws as

$$z^2 - (3\pi/4)z + 1 = 0 \tag{21}$$

It can then be shown from Eq. (21) that Burt's steering law (transverse steering) is only more efficient than that of Pollard (major axis steering) for an eccentricity greater than 0.832.

For chemical propulsion, the optimum maneuver to increase the orbit argument of perigee, while leaving the other orbital elements unchanged, consists of two equal impulses applied to connect the initial and rotated orbits through the arc of an intermediate transfer ellipse. It can be shown that the change in arguement of perigee obtained in a single orbit through the application of two impulses of total magnitude Δv is given by[10]

$$\Delta\omega = (2/e)\sqrt{a(1 - e^2)/\mu}\,\Delta v \tag{22}$$

Note that the analysis by Pollard,[8] which provides a single impulse at the intersection of the initial and rotated orbits, is not optimal for an eccentricity of less than 0.775. To obtain sun-synchronous precession of the apse line, the change in argument of perigee over a single orbit must be $\Delta\omega = \dot{\lambda}_S T_0$, where again $T_0 = 2\pi\sqrt{(a^3/\mu)}$ is the ellipse orbit period. The required Δv per orbit for sun-synchronous apse-line precession for chemical propulsion is then obtained as

$$\Delta v = \pi\dot{\lambda}_S\left[ae/\sqrt{(1 - e^2)}\right] \tag{23}$$

which can then be used to determine the accumulated Δv for some total mission duration.

To make an approximate comparison of solar sail and electric and chemical propulsion, an assessement of the effective Δv and propellant mass fractions required will be made for the 10×30 Earth radii mission orbit. Because the orbit eccentricity is 0.5, the steering law derived from Pollard (major axis steering) is the most appropriate for electric propulsion and the two-impulse maneuver is optimum for chemical propulsion. The effective Δv and propellant mass fraction ($\Delta m/m_0$) for one year of operation are shown in Table 1, assuming an electric propulsion system specific impulse of 3000 s and a chemical propulsion system specific impulse

Table 1 Requirements for sun-synchronous apse-line precession of a 10 × 30 Earth radii mission orbit over one year of operation

Propulsion system	Δv, km/s	$\Delta m/m_0$
Solar sail	—	—
Electric ($I_{sp} = 3000$ s)	4.29	0.14
Chemical ($I_{sp} = 340$ s)	3.21	0.62

of 340 s, typical of a bipropellant hydrazine system. These mass fractions are calculated using the rocket equation and assume the effective Δv for the electric propulsion system is found from the product of the required acceleration [from Eq. (9)] and the mission duration. It can be seen that the propellant mass fraction is rather large for chemical propulsion, but is more modest for electric propulsion. A more detailed analysis of these competing modes of propulsion will be required to reach stronger conclusions regarding the optimum mode of propulsion. However, for long-duration, multiyear missions, solar sailing is likely to show significant benefits.

Locally Optimum Apse-Line Precession

Although the steering laws discussed for solar sail and electric propulsion are simple to implement, they are not optimum. In this section, a set of locally optimum steering laws that maximize the instantaneous rate of change of argument of perigee are defined. First, the locally optimum steering law for an electric propulsion system will be investigated and then adapted for use by a solar sail.

For an electric propulsion system, the thrust vector will be assumed to act in the orbit plane at some angle ϕ relative to the radial direction, as shown in Fig. 1. The perturbing acceleration $\boldsymbol{a}_p$ due to the low-thrust propulsion system is then given in component form by

$$\begin{bmatrix} R \\ T \end{bmatrix} = a_p \begin{bmatrix} \cos\phi \\ \sin\phi \end{bmatrix} \tag{24}$$

When these components of the perturbing low-thrust acceleration are substituted into Eq. (3), the instantaneous rate of change of argument of perigee is maximized if

$$\frac{\partial}{\partial\phi}\left[-a_p\cos\phi\cos f + a_p\sin\phi\left(1+\frac{r}{p}\right)\sin f\right] = 0 \tag{25}$$

Equation (25) is solved for the required thrust angle as a function of true anomaly and yields a locally optimum steering law

$$\tan\tilde{\phi} = -\left(\frac{2+e\cos f}{1+e\cos f}\right)\tan f \tag{26}$$

where $\tilde{\phi}$ is the optimum thrust angle. It is found that due to the symmetry of this new steering law the orbit-averaged semimajor axis and eccentricity again remain unchanged while the apse line of the orbit precesses. The required thrust angle relative to the sun line is shown in Fig. 4 for the 10 × 30 Earth radii mission orbit. It can be seen that the locally optimum steering law differs somewhat from the simpler steering law in which the thrust vector is directed along the sun line. For the 10 × 30 Earth radii mission orbit, it is found that the acceleration required from the low-thrust propulsion system is reduced from 0.136 to 0.127 mm/s^2 using this new steering law. The corresponding effective Δv is reduced from 4.29 to 4.01 km/s.

To obtain a locally optimum steering law for a solar sail, it is now necessary to choose the sail orientation such that the component of solar radiation pressure acceleration along the direction defined by Eq. (26) is maximized. The steering law defined by Eq. (26) provides the thrust angle relative to the radial direction. Relative to the sun line, this direction is defined by $\tilde{\alpha} = \tilde{\phi} - (\pi - f)$, as can be seen from Fig. 1. Therefore, the component of solar radiation pressure acceleration in this direction is given by

$$\tilde{a} = a_0\cos^2\alpha\cos(\alpha - \tilde{\alpha}) \tag{27}$$

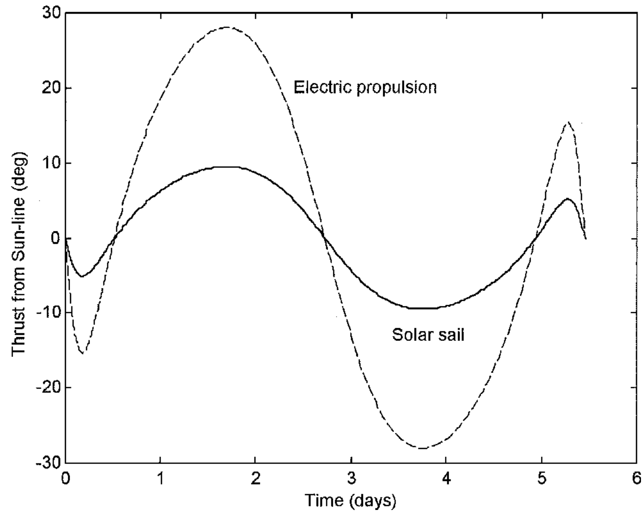

Fig. 4 Optimum thrust pointing relative to the sun line for a 10 × 30 Earth radii mission orbit over 1 orbit period [——, solar sail equation (29) and – – –, electric propulsion equation (26)].

To optimize the solar sail steering law, it is now required that $\partial\tilde{a}/\partial\alpha = 0$, so that

$$2\sin\alpha\cos(\alpha - \tilde{\alpha}) + \cos\alpha\sin(\alpha - \tilde{\alpha}) = 0 \tag{28}$$

After some manipulation, it can be shown that Eq. (28) may be reduced to a polynomial with solution

$$\tan\alpha^* = \frac{-3 + \sqrt{9 + 8\tan^2\tilde{\alpha}}}{4\tan\tilde{\alpha}} \tag{29}$$

where α^* is the locally optimum sail steering angle. Equation (29) represents the direction of the sail normal relative to the sun line to maximize the instantaneous rate of change of argument of pericenter.

Again, it is found that due to the symmetry of this new steering law the orbit averaged semimajor axis and eccentricity remain unchanged while the apse line of the orbit precesses. The required optimum sail pitch angle relative to the sun line is also shown in Fig. 4 for the 10 × 30 Earth radii mission orbit. It is clear that the locally optimum steering law for the solar sail is close to the simple steering law in which the sail normal is directed along the sun line. For sun-synchronous precession of the orbit apse line, it is found that the required sail characteristic acceleration is reduced somewhat from 0.136 to 0.129 mm/s^2 for the 10 × 30 Earth radii mission orbit by using the optimum steering law.

GEOSAIL Mission

It has been shown that to artificially precess the apse line of an elliptical orbit in a sun-synchronous manner requires only a constant acceleration directed along the major axis of the ellipse. A 10 × 30 Earth radii elliptical orbit used for a geomagnetic tail mission would require an effective Δv of order 3.2 km/s per year of operation for apse-line precession. Although the Δv for apse-line precession for this orbit is large, it has been shown that only a relatively small acceleration is in principle necessary. For a solar sail, it was found that a characteristic acceleration of 0.138 mm/s^2 is required for the 10 × 30 Earth radii mission orbit, including eclipse periods. Because the precession of the apse line of the orbit is chosen to match that of the sun line, the sail normal can be directed along the sun line. Such a simple steering law has significant operational advantages because a sun-facing attitude can be achieved passively by configuring the sail to be slightly conical such that its center of pressure lies behind its center of mass.[11]

A small geomagnetic tail mission can in principle be delivered to a 10 × 30 Earth radii orbit using the solar sail to spiral from a piggyback launch, for example, to geostationary transfer orbit (GTO). For a standard Ariane V midnight launch to GTO, the apse line of the orbit is directed sunward, opposite to the geomagnetic tail. A 6-month (or 18-month) orbit raising phase is, therefore, required while the solar sail maneuvers to the required operational orbit, and the apse line aligns with the geomagnetic tail. During this time, the orbit plane must also be rotated so that the orbit lies in the ecliptic plane. The final GEOSAIL mission orbit is shown in Fig. 5 (Ref. 12).

An alternative launch scenario to piggy-back delivery to GTO would inject the packaged sail and spacecraft bus directly into the operational 10×30 Earth radii orbit in the ecliptic plane using a dedicated launcher or a piggy-back launch with chemical kick stages. In this scenario, if sail deployment was to fail, the spacecraft bus could be separated and would perform a conventional geomagnetic tail mission without apse-line precession. In this case, the mission is only degraded and not lost in the event of a deployment failure. The risk of using solar sail technology on a first mission is then significantly reduced because a useful backup mission is available without the use of the sail. In addition, because the sun-pointing steering law can be implemented by passive means, the solar sail does not require active attitude control if directly injected to the

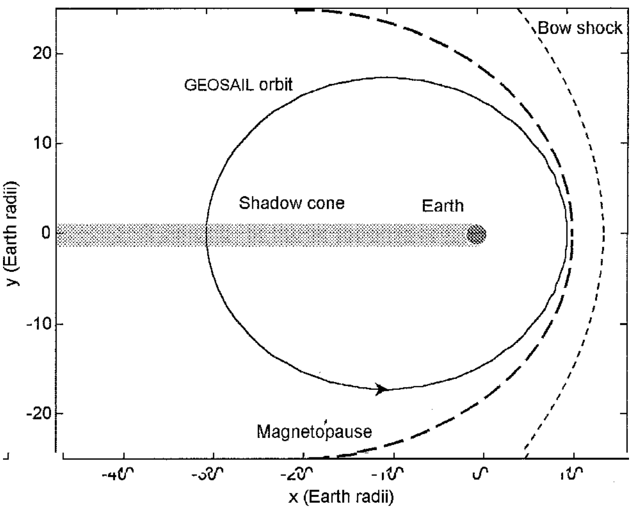

Fig. 5 GEOSAIL mission orbit.

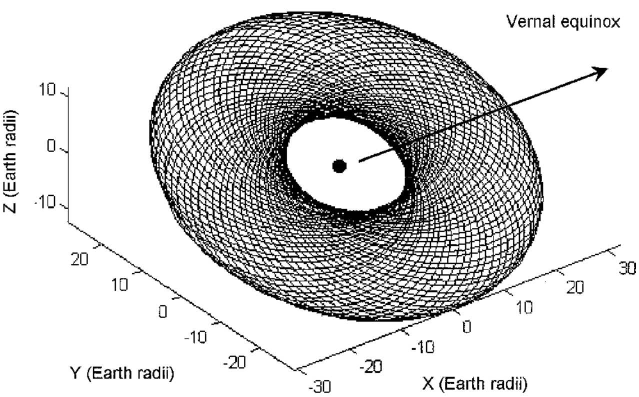

Fig. 6a GEOSAIL orbit evolution with luni–solar perturbations over 1 year in Earth-centered inertial axes.

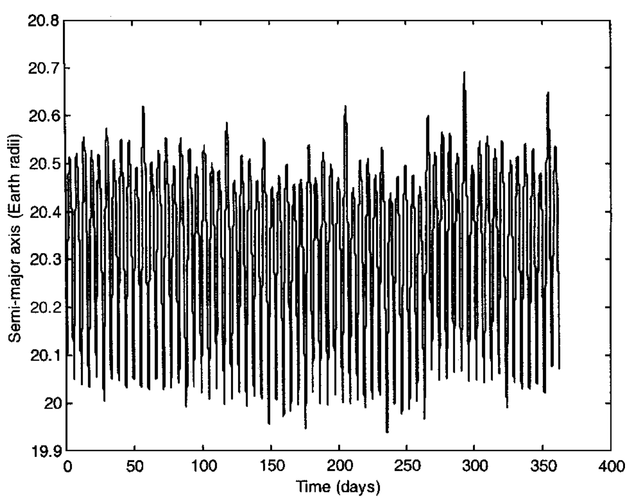

Fig. 6b GEOSAIL orbit semimajor axis.

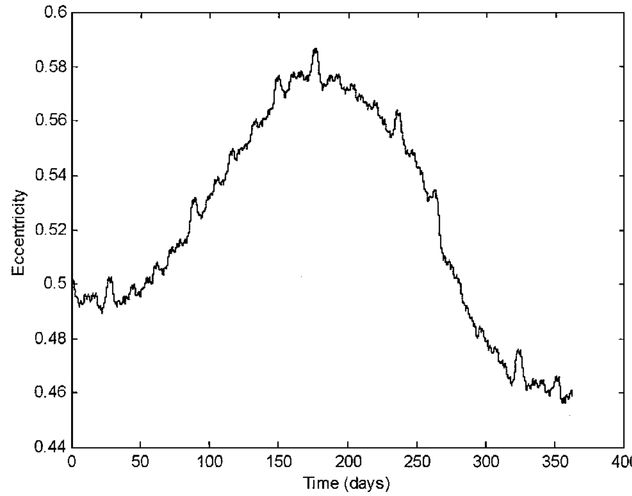

Fig. 6c GEOSAIL orbit eccentricity.

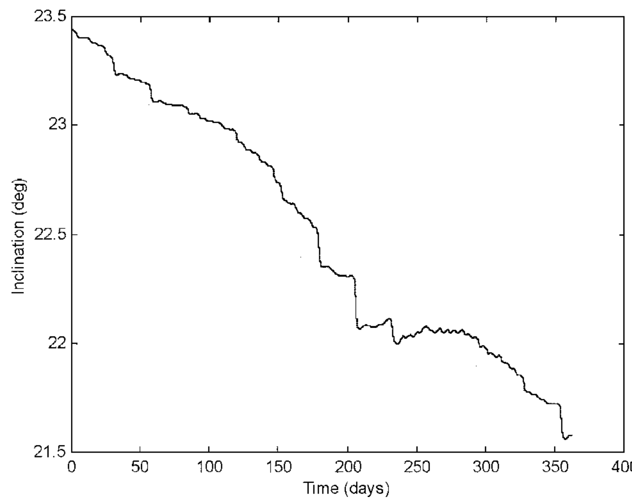

Fig. 6d GEOSAIL orbit inclination.

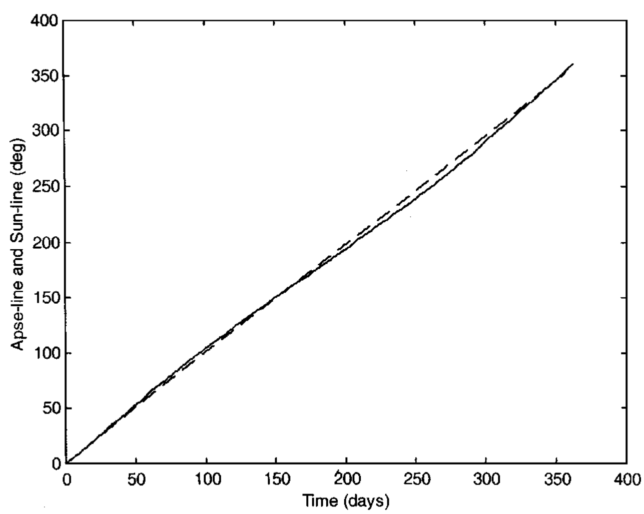

Fig. 6e GEOSAIL apse line ω (——) and sun line λ_S (- - -) over 1 year.

Table 2 Strawman instrument mass budget

Instrument	Mass, kg	Science goal
Flux-gate magnetometer	0.2	High-resolution magnetic field measurements
Electrostatic analyser	2.0	Electron and ion distribution
Data processor	0.2	
Solid state telescope	0.6	Energetic particle mass and distribution functions
Data processor	0.1	
Search-coil magnetometer	1.3	Rapid variations of magnetic field in interaction region between solar wind and magnetosphere
Data processor	0.6	
Total mass	5.0	
Total power	5 W	

Table 3 Spacecraft mass budget for a 1444 m^2 solar sail with a characteristic acceleration of 0.138 mm/s^2

Mass contribution	Mass, kg
Instruments	5
Spacecraft bus	25
Solar sail	
Booms (100 g/m)	11
Mechanisms	20
Film (7.5-μm Kapton)	15
Coatings (0.1-μm aluminum)	0.5
Bonding	2.5
Launch adapter	1
Launch mass	80

mission orbit and so can be a simple conical deployable reflector attached to the spacecraft bus.

The GEOSAIL mission concept provides a useful science return that is absent from other concepts for solar sail technology demonstration missions, such as a slow spiral from GTO to escape or a lunar fly-past. As such, it provides an early opportunity to combine technology demonstration with a novel and extremely useful science mission. Most science applications of solar sailing center on deep space missions, which require a launch capacity to Earth escape and the use of deep space network (DSN) facilities. This Earth-orbiting application allows low-cost launch and low-cost ground facilities.

When active maneuvering or a direct launch to the 10×30 Earth radii orbit in the ecliptic plane is assumed, the simple sun-pointing steering law provides close tracking of the geomagnetic tail. A simulation of the sun-pointing steering law is shown in Fig. 6 for the 10×30 Earth radii mission orbit over a 12-month period, including lunar and solar gravitational perturbations and an order 12×12 geopotential model. A fourth-order Runge–Kutta integrator is used in Earth-centerd inertial coordinates. The mission is assumed to begin at the spring equinox (21 March 2001) with an equatorial inclination of 23.4 deg, corresponding to an orbit within the ecliptic plane. It can be seen that the sun line is closely tracked in the presence of these perturbations, although long-period forcing of the orbit eccentricity is observed, along with a slow secular perturbation to the orbit inclination due to lunar and solar gravitational perturbations.

To size a solar sail for the GEOSAIL mission a 25-kg spacecraft bus and 5-kg instrument payload will be defined. This is typical of concepts for minisatellites with a suite of simple field and particle instruments.[13] A strawman instrument payload has been defined to meet the science goals of the mission, the mass budget for which is shown in Table 2. The instrument suite is representative of current high time resolution plasma detectors and low mass electric field detectors required to characterize the geomagnetic tail plasma. The sail film is assumed to be fabricated from commercially available 7.5-μm Kapton® film, vapor coated with aluminum. An additional fraction of the sail film mass is added to account for bonding of elements of the sail and for micrometeorite rip stops. The sail booms can be deployable carbon-fiber (CFRP) profiles,[6] bistable composite shells,[14] or space-rigidized inflatables.[15] When booms are assumed with a specific mass of 100 g/m, typical of current technology,[6] a spacecraft mass budget can be defined, as shown in Table 3. The sail is assumed to have a total reflectivity of 85% and so has an area of 1444 m^2 and a total launch mass of 80 kg providing the required sail characteristic acceleration of 0.138 mm/s^2. This launch mass is within the 100-kg limit for launch as an Ariane V auxiliary payload.

In addition to a single 30-kg spacecraft, the GEOSAIL concept may be adapted to enhance existing concepts for constellations of microspacecraft, each with a mass of order 1 kg (Ref. 16). These microspacecraft are envisaged as acting as distributed nodes of a network of sensors to map the spatial and temporal characteristics of the geomagnetic tail. For a constellation of 1-kg microspacecraft distributed around a 10×30 Earth radii orbit, a 5×5 m solar sail with a mass of order 0.8 kg is required. Here, the constellation would be injected directly into the mission orbit using chemical propulsion so that the sail would be a simple deployable reflector attached to each microspacecraft and functionally separate from the spacecraft bus and payload. Because only a simple sun-pointing steering law is required, active attitude control of the sail is not required, and the sail can be configured to be conical in form to provide passive attitude stabilization, as discussed earlier.[11]

Conclusions

It has been shown that a small, low-performance solar sail can be used to artificially precess the apse line of an elliptical orbit to provide sun-synchronous tracking of the geomagnetic tail. Such sun-synchronous precession is of practical interest to enable space physics missions in which the science payload is kept within the geomagnetic tail during the entire mission. This strategy is in contrast to conventional geomagnetic tail missions in which the apse line of the mission orbit only coincides with the sun line once per year. Although such apse-line precession can be achieved using chemical or electric propulsion, the Δv is large for chemical propulsion. For electric propulsion, the requirement for reaction mass is likely to limit the duration for which sun-synchronous apse-line precession can be achieved. However, more detailed trade studies are required to allow a direct comparison of electric propulsion and solar sailing. In conclusion though, the use of a small, low-performance solar sail is seen as an effective means of enabling a novel space science mission while acting as a demonstration mission for solar sail propulsion.

Acknowledgments

This work was partly supported by funding from the Lockheed Martin Advanced Technology Center (Order SXCDA5101F). The possibility of using a solar sail to precess the apse line of an elliptical orbit was raised during informal discussions with Robert Lin (University of California, Berkeley, Space Sciences Laboratory).

References

[1] McInnes, C. R., *Solar Sailing: Technology, Dynamics and Mission Applications*, Springer-Verlag, London, 1999, pp. 19–31.

[2] McInnes, C. R., "Solar Sail Mission Applications for Non-Keplerian Orbits," *Acta Astronautica*, Vol. 45, Nos. 5–9, 1999, pp. 567–575.

[3] McInnes, C. R., "Artificial Lagrange Points for a Non-Perfect Solar Sail," *Journal of Guidance, Control, and Dynamics*, Vol. 22, No. 1, 1999, pp. 185–187.

[4] Leipold, M., and Wagner, O., "Mercury Sun-Synchronous Polar Orbits Using Solar Sail Propulsion," *Journal of Guidance, Control, and Dynamics*, Vol. 19, No. 6, 1996, pp. 137–141.

[5] Gombosi, T. I., *Physics of the Space Environment*, Cambridge Univ. Press, Cambridge, England, U.K., 1998, pp. 278–312.

[6] Garner, C., and Leipold, M., "Developments and Activities in Solar Sail Propulsion," AIAA Paper 2000-3858, July 2000.

[7] Fortescue, P., and Stark, J., *Spacecraft Systems Engineering*, Wiley, New York, 1995, pp. 89, 90.

[8] Pollard, J. E., "Evaluation of Low-Thrust Orbital Manoeuvres," AIAA Paper 98-3486, July 1998.

[9] Burt, E. G. C., "The Dynamics of Low-Thrust Spacecraft Manoeuvres," *Journal of the Royal Aeronautical Society*, Vol. 72, No. 695, 1968, pp. 925–940.

[10] Mishne, D., Melamed, N., and Shinar, J., "Aeroassisted Transfer Between Elliptical Orbits Using Lift Control," *Journal of Guidance, Control, and Dynamics*, Vol. 13, No. 5, 1990, pp. 785–791.

[11] Sohn, R., "Attitude Stabilisation by Means of Solar Radiation Pressure," *ARS Journal*, Vol. 29, No. 5, 1959, pp. 371–373.

[12]Macdonald, M., and McInnes, C. R., "Geosail: An Enhanced Magnetospheric Mission Using a Small Low Cost Solar Sail," 51st International Astronautical Federation Congress, IAF Paper 00-W.1.06, Oct. 2000.

[13]Schwartz, S. J., Balough, A., Cargill, P., Fazakerley, A. N., and Johnstone, A. D., "SWARM: A Fleet of Microsatellites to Explore the Magnetosphere," *Science Closure and Enabling Technologies for Constellation Class Missions*, edited by V. Angelopoulos and P. V. Panetta, Univ. of California, Berkeley, CA, 1998, pp. 63–65.

[14]Iqbal, K., and Pellegrino, S., "Bi-Stable Composite Shells," AIAA Paper 2000-1385, April 2000.

[15]Freeland, R. E., Bilyev, G. D., Veal, G. R., Steiner, M. D., and Carson, D. E., "Large Inflatable Deployable Antenna Flight Experiment Results," 48th International Astronautical Federation Congress, IAF Paper 97-1.3.01, Oct. 1997.

[16]Petschek, H. E., Rayburn, C., Sheldon, R., Vickers, J., Bellino, M., Bevis, G., and Spence, H. E., "The Kilo-Satellite Constellation Concept," *Science Closure and Enabling Technologies for Constellation Class Missions*, edited by V. Angelopoulos and P. V. Panetta, Univ. of California, Berkeley, CA, 1998, pp. 63–65.

C. A. Kluever
Associate Editor